arXiv:1310.3813v1 [cond-mat.supr-con] 14 Oct 2013

Superconductivity in Graphene-Lithium

D. M. Guzman*

School of Materials Engineering, Purdue University,

West Lafayette, Indiana 47907, USA

H. M. Alyahyaei†

Department of Materials Science and Engineering,

University of California, Riverside, California 92521, USA

R. A. Jishi‡

Department of Physics and Astronomy,

California State University, Los Angeles, California 90032, USA

We present first-principles calculations on systems consisting of a few layers of graphene and lithium. In particular, we investigate the evolution of the electron-phonon coupling strength with increasing number of layers. We find that, for intercalated systems such as C_6-Li-C_6 or C_6-Li-C_6-Li-C_6, the electron-phonon coupling is weak. However, for systems of equal number of graphene and lithium layers, such as C_6-Li or C_6-Li-C_6-Li, the electron-phonon coupling is strong. We investigate the optimal configuration that yields the highest superconducting transition temperature.

PACS numbers: 71.15.Mb, 63.22.Rc, 73.22.Pr, 74.78.-w

Keywords: graphene intercalates, electron-phonon coupling, superconductivity.

I. INTRODUCTION

Ever since its discovery, graphene[1] has shown a great potential for applications in nano-technology[2–5], especially in electronic transport[6]. Studies of superconductivity in graphite intercalation compounds (GICs)[7–16], recent experimental evidence of a su-

*Electronic address: guzmand@purdue.edu

†Electronic address: halya001@ucr.edu

‡Electronic address: rjishi@calstatela.edu; Corresponding author

perconducting state in graphite-sulfur composites[17, 18], and the growing interest in superconducting nano-devices[19–21] have motivated theoretical investigation of possible superconductivity in the two-dimensional graphene systems[22–28]. Single- and few-layer graphene may exhibit a superconducting state upon adatom deposition or intercalation. As in the case of alkali-metal and alkaline-earth GICs, superconductivity in modified-graphene systems can be explained by the electron-phonon coupling enhancement that arises from the presence of an intercalant-derived band as well as graphitic π-bands at the Fermi level[12, 29, 30].

Theoretical studies within the density functional theory (DFT) framework were conducted on single- and few-layer graphene systems with intercalated and deposited dopants. The electron-phonon coupling parameter λ was found to be 0.60 and 0.80, respectively, in calcium intercalated graphene bilayers and trilayers. The superconducting transition temperature T_c was estimated to be 4.1 K for Ca-intercalated bilayer and 10.1 K for Ca-intercalated trilayer[31]. Recently, the possibility of a superconducting state in lithium covered graphene monolayers was discussed by Profeta *et al.* [32]. They argued that removal of quantum confinement, in going from LiC_6 GIC to Li-covered monolayer graphene, could bring the Li-derived states down in energy to the Fermi level. This enhances the electron-phonon coupling strength, making Li-covered single-layer graphene a superconductor at $T_c = 8.1$ K.

The recent fabrication of lithium intercalated graphene bilayer [33] raises the question of whether this two-dimensional material would also exhibit a superconducting state. In addition, the possibility of a further enhancement of the electron-phonon coupling strength in few-layer graphene systems intercalated with lithium, remains an open issue.

In this work, we study the effect of increasing number of Li-doped graphene layers on the electron-phonon coupling strength via first-principles density functional theory. Details of our methods are presented in Section III. The electronic structure of lithium covered graphene and lithium intercalated graphene layers is calculated. It is found that only Li-covered graphene systems exhibit a coexistence of Li-derived s-bands and graphitic π-bands at the Fermi level. In the case of Li-intercalated graphene systems, the interlayer band (derived from Li states) is unoccupied. From the vibrational modes and electron-phonon coupling calculations we find that a significant coupling of electrons to out-of-plane vibrations is necessary to achieve a significant enhancement of the total electron-phonon

coupling strength.

In Section II we describe the crystal structure of the Li-doped graphene systems investigated in this work, and in Section III details of the methods of calculation are presented. The results of the electronic structure and vibrational modes calculations are presented and discussed in Section IV and V, respectively. Conclusions are given in Section VI.

II. CRYSTAL STRUCTURE

Systems consisting of equal numbers of graphene and lithium layers (Li-covered graphene) and lithium intercalated graphene layers were systematically analyzed from first-principles. Calculations of the electronic structure and vibrational modes were carried out on systems of up to four lithium and four graphene layers for Li-covered graphene and up to two lithium and three graphene layers for Li-intercalated graphene layers. In all the cases considered, the unit cell is a $(\sqrt{3}a \times \sqrt{3}a)$ R 30° supercell of the graphene sheet unit cell. In agreement with the stage-1 Li-GIC, the carbon layer stacking is taken to be $AAAA$. The separation between adjacent carbon and Li layers is set at 1.855 Å, similar to the corresponding value in Li GICs. The in-plane lattice constants are $a = b = 4.33$ Å. Since the DFT calculations are carried out on a 3-dimensional crystal, the c-lattice constant is taken to be sufficiently large so as to render the system, in effect, two-dimensional.

For systems of the form C_6-Li-C_6-Li and C_6-Li-C_6-Li-C_6, two stacking configuration for the Li layers were considered. In one configuration, Li atoms in both layers sit above the hollow sites of the graphene layer which are labeled α (see Fig. 1). The stackings for C_6-Li-C_6-Li and C_6-Li-C_6-Li-C_6 are $A\alpha A\alpha$ and $A\alpha A\alpha A$, respectively. In this configuration, C_6-Li-C_6-Li and C_6-Li-C_6-Li-C_6 will be simply denoted as $C_6Li_{\alpha\alpha}$ and $C_6Li_{\alpha\alpha}C_6$, respectively. In the other configuration, whereas the Li atoms between the first and second graphene layers occupy positions labeled α, the Li atoms above the second carbon layer occupy positions labeled β. In this case, the two Li layers are not directly above each other; the second layer is shifted, relative to the first, by a lattice vector of the graphene sheet. In this configuration, the stacking sequence is $A\alpha A\beta$ for the Li-covered system, and $A\alpha A\beta A$ for the intercalated system. In this configuration, the Li-covered system will be denoted as $C_6Li_{\alpha\beta}$, while the intercalated system will be written as $C_6Li_{\alpha\beta}C_6$.

For structures with three Li layers, two stacking configurations were considered. The

first, in which the three Li layers are directly above each other, is $A\alpha A\alpha A\alpha$. The corresponding system, C_6-Li-C_6-Li-C_6-Li, will be denoted as $C_6Li_{\alpha\alpha\alpha}$. In the second configuration, the Li atoms between the first and second graphene layers occupy the hollow sites labeled α, those between the second and third graphene layers sit in hollow sites labeled β, and those above the third graphene layer occupy sites labeled γ. The third layer of Li adatoms is shifted, relative to the second Li layer, by a lattice vector of the graphene sheet. The stacking is of the form $A\alpha A\beta A\gamma$, and the Li-covered system is denoted by $C_6Li_{\alpha\beta\gamma}$.

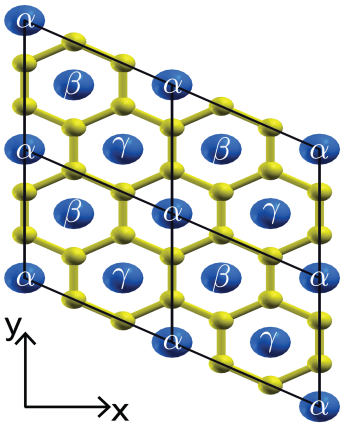

FIG. 1: (Color online) The graphene sites labeled α, β, and γ. In the Li-covered system denoted by $C_6Li_{\alpha\beta\gamma}$, Li atoms sit over the α-sites of the first graphene sheet, over the β-sites of the second graphene sheet, and over the γ-sites of the third graphene sheet.

III. METHODS

The reported total energy and electronic structure were obtained from density functional theory (DFT) calculations using the all-electron, full-potential, linear augmented plane wave (FP-LAPW) method as implemented in the WIEN2K code [34]. The exchange-correlation potential was calculated using the generalized gradient approximation (GGA) as proposed by Perdew, Burke, and Ernzerhof [35]. The radii of the muffin-tin spheres for the carbon and lithium atoms were taken as $1.36a_0$ and $2.21a_0$, respectively, where a_0 is the Bohr radius. The product $R_{MT}K_{max}$ was set to 7, where R_{MT} is the smallest muffin-tin radius and K_{max} is a cutoff wave vector. The valence electrons wave functions inside the muffin-tin spheres were expanded in terms of spherical harmonics up to $l_{max} = 10$, and in

terms of plane waves with a cutoff wave vector K_{max} in the interstitial region. The charge density was Fourier expanded up to a maximum wave vector $G_{max} = 13a_0^{-1}$. Convergence of the self-consistent field calculations was attained with a total energy convergence tolerance of 0.1 mRy and a total charge convergence tolerance of 0.0001 e.

The frequencies of the vibrational modes and the electron-phonon coupling parameter were calculated using the QUANTUM-ESPRESSO[36] package with norm-conserving pseudopotentials. The valence electrons wave functions and the charge density were expanded in plane waves using 40 Ry and 300 Ry energy cutoffs, respectively. The phonon frequencies were calculated within the linear-response framework on an $8 \times 8 \times 1$ phonon-momentum mesh with a $16 \times 16 \times 1$ uniform electron-momentum mesh. For the calculation of the electronic density of states and the electron-phonon coupling strength, a uniform $40 \times 40 \times 1$ **k**-point mesh in the Brillouin zone was used.

The Eliashberg spectral function $\alpha^2F(\omega)$ is given by

$$\alpha^2F(\omega) = \frac{1}{N(0)N_kN_q} \sum_{n\mathbf{k},m\mathbf{q},\nu} |g^{\nu}_{n\mathbf{k},m\mathbf{k}+\mathbf{q}}|^2 \times \delta(\varepsilon_{n\mathbf{k}})\delta(\varepsilon_{m\mathbf{k}+\mathbf{q}})\delta(\hbar\omega - \hbar\omega^{\nu}_{\mathbf{q}}) \tag{1}$$

where $N(0)$ is the total density of states at the Fermi level, and N_k and N_q are the total number of **k**- and **q**-points, respectively. In the above equation, $\varepsilon_{n\mathbf{k}}$ is the energy, measured from the Fermi level, of an electron with wave vector **k** in energy band n, $\omega^{\nu}_{\mathbf{q}}$ is the frequency of a phonon with wave vector **q** and branch index ν, and $g^{\nu}_{n\mathbf{k},m\mathbf{k}+\mathbf{q}}$ is the matrix element of the electron-phonon interaction.

The coupling strength of electrons to all phonon modes with frequencies below ω is defined as

$$\lambda(\omega) = 2\int_0^{\omega} \frac{\alpha^2F(\omega')}{\omega'}\, d\omega' \tag{2}$$

The total electron-phonon coupling is calculated as $\lambda(\omega \to \infty)$. The values of the superconducting transition temperature were computed using the Allen-Dynes [37] modification of the McMillan formula [38],

$$kT_c = \frac{\hbar\omega_{log}}{1.2} exp\left[\frac{-1.04(1+\lambda)}{\lambda - \mu^*(1+0.62\lambda)}\right] \tag{3}$$

where ω_{log} is the phonon logarithmic average frequency. The screened Coulomb pseudopotential [39] μ^* was taken as 0.115.

IV. ELECTRONIC STRUCTURE

In Figures 2 and 3 we present the energy band dispersion and density of states (DOS) of lithium-covered graphene layer (C_6Li) and lithium-intercalated graphene bilayer (C_6LiC_6), respectively. By inspection of the band-structure of C_6LiC_6, we notice that the interlayer band (derived from Li states) at the Fermi level is empty, as is the case in stage-1 Li-GIC, which is not a superconductor. In the case of C_6LiC_6, the *c*-direction confinement, imposed by the top and bottom graphene layers, keeps the interlayer band from being occupied. As Figure 3a reveals, the bottom of the Li-derived band is ~ 1.75 eV above the Fermi energy. Based on these grounds, any further increase in the number of layers will not create new Li-derived states at the Fermi level.

In the case of Li-covered graphene, we see that the Fermi level is crossed by an *s*-band derived from Li states. The removal of the top graphene layer has the effect of bringing down the energy of the Li-derived band to the Fermi level; this suggests that there is a partial charge transfer from the Li atoms to the carbon sheet. The amount of charge transferred from each Li atom is calculated using Bader's quantum theory of "atoms in molecules" [40], and the results are presented in Table I. The table reveals that there are two values of the charge transfer: 0.69 electrons (partial transfer) from an Li atom in the outer layer, and 0.88 electrons (almost complete transfer) from an Li atom in an inner layer surrounded by two graphene layers. As in the case of GICs [41], the presence of an adatom band at the Fermi level increases the number of carriers, promotes electron coupling to the low energy carbon atoms out-of-plane vibrations, and generates coupling to the adatom vibrations. [42].

In Figure 2(c) the partial density of states (PDOS) and the total DOS of C_6Li are compared. The total density of states is the sum of the atomic densities of states and the density of states in the interstitial region. It is important to note that the Li-projected DOS comes predominantly from the *s*-band. The LAPW method projects the DOS onto the muffin-tin spheres, yielding the atomic densities of states; the rest of the total DOS is assigned to the interstitial region. Figure 2c shows that a substantial portion of the DOS results from the interstitial region. Since the interstitial space in this structure is mainly the space between the Li muffin-tin spheres, the contribution of the Li-derived *s*-band to the total DOS is comparable to that from the graphitic π bands.

TABLE I: Charge transfer (e^- per Li atom) from lithium atoms to graphene planes calculated using Bader's "atoms in molecules" (AIM) method for selected systems. For the Li-covered graphene systems with more than one lithium layer, the reported charge transfer is from Li atoms in the outer layer.

Structure	Charge Transfer (e^-/Li)	Structure	Charge Transfer (e^-/Li)
C_6Li	0.6847	$C_6Li_{\alpha\beta}$	0.6931
$C_6Li_{\alpha\alpha}$	0.6922	$C_6Li_{\alpha\beta\gamma}$	0.6892
$C_6Li_{\alpha\alpha\alpha}$	0.6898	C_6LiC_6	0.8784
$C_6Li_{\alpha\alpha\alpha\alpha}$	0.6894	$C_6Li_{\alpha\beta}C_6$	0.8803

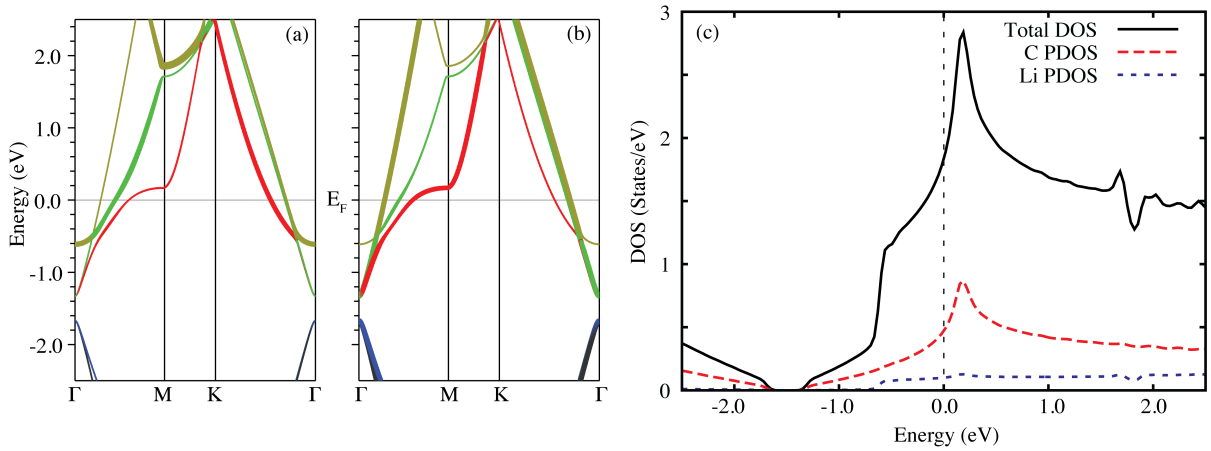

FIG. 2: (Color online) Plot of the energy bands ((a) and (b)) and density of states (c) in Li-covered graphene layer C_6Li along high symmetry directions in the Brillouin zone. The width of the bands at every **k**-point is proportional to the contribution of (a) Li-derived states, and (b) C-derived states. The Fermi level is set at zero energy.

We now focus on Li-covered and Li-intercalated graphene systems with two and three lithium layers. As discussed before (Sec. II), we considered two stacking configurations when dealing with more than one lithium layer.

The first issue to address is to determine which stacking configuration yields a more stable structure. To study this, we carried out total energy calculations for the Li-covered and the Li-intercalated systems considered in this work. In all cases, we found that the lowest energy is obtained when the Li atoms of different layers sit directly above each other, so the Li layers are not shifted with respect to each other. In the case of Li-covered graphene layers, the structure $C_6Li_{\alpha\alpha}$ is lower in energy than its counterpart $C_6Li_{\alpha\beta}$ by

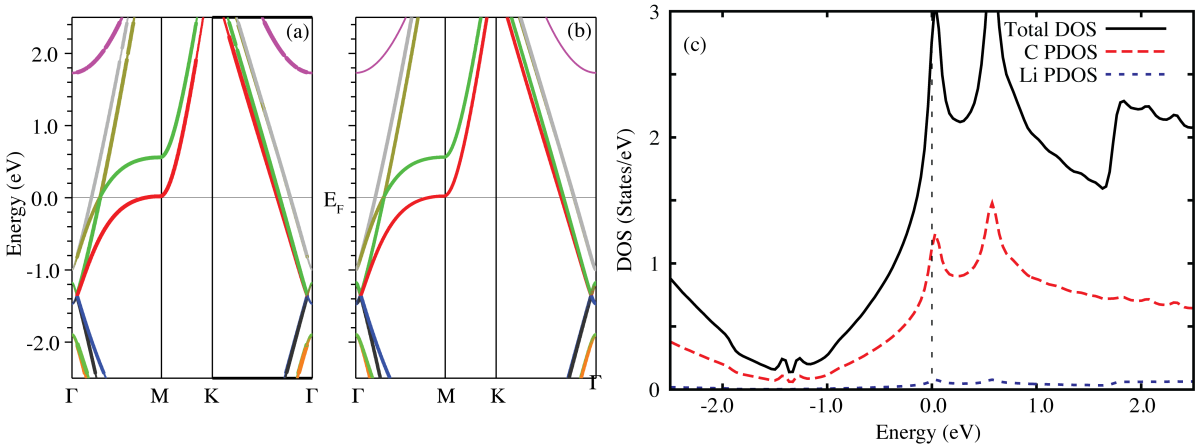

FIG. 3: (Color online) Plot of the energy bands ((a) and (b)) and density of states (c) in Li-intercalated graphene bilayer C_6LiC_6 along high symmetry directions in the Brillouin zone. The width of the bands at every **k**-point is proportional to the contribution of (a) Li-derived states, and (b) C-derived states. The Fermi level is set at zero energy.

19.45 meV per unit cell, the energy of $C_6Li_{\alpha\alpha\alpha}$ is lower than $C_6Li_{\alpha\beta\gamma}$ by 41.95 meV per unit cell. In the case of Li-intercalated graphene layers, the structure $C_6Li_{\alpha\alpha}C_6$ is lower in energy than $C_6Li_{\alpha\beta}C_6$ by 20.42 meV per unit cell.

Although it is concluded that it is energetically favorable for the lithium atoms of different layers to sit in equivalent hollow sites (Li stacking $\alpha\alpha\alpha$), there is some experimental evidence (Ref. [43] and references therein) that at low temperatures the lithium intercalant layers in stage-1 LiC_6 GIC are sequentially arranged as $\alpha\beta\gamma$. For this reason we continue the comparative study of all structures regardless of their stacking configuration.

Figure 4 shows the calculated band structure and DOS of $C_6Li_{\alpha\beta}$. In similarity to the the C_6Li monolayer case, there is a lithium s-band as well as graphitic π-bands crossing the Fermi level simultaneously. We note that the s-band is derived from orbitals of the Li atoms lying in the outer Li layer. We also note that there is a substantial increase in the density of states at the Fermi level in comparison with the C_6Li case. In the $C_6Li_{\alpha\beta}$ unit cell, there are two inequivalent Li atoms and two inequivalent C atoms. The atomic densities of states shown in Fig. 4 are for the outer layer Li atoms and the C atoms in the adjacent layer.

We have also calculated the electronic structure of $C_6Li_{\alpha\beta\gamma}$ (plots of the energy bands

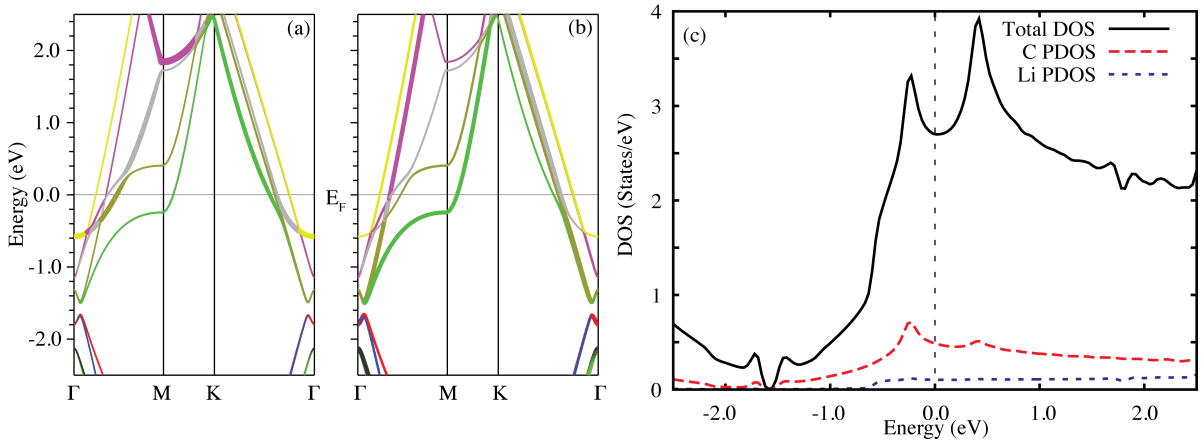

FIG. 4: (Color online) Plot of the energy bands ((a) and (b)) and density of states (c) in Li-covered graphene $C_6Li_{\alpha\beta}$ along a high symmetry path in the Brillouin zone. The width of the bands in (a) is proportional to the the contribution of the orbitals of the outer Li layer, while in (b) it is proportional to the contribution of the orbitals of the carbon atoms in the graphene layer adjacent to the outside Li layer. The Fermi level is set at zero energy.

and DOS for this structure are provided in the supplementary material). As expected from the previous case ($C_6Li_{\alpha\beta}$), in addition to the graphitic π-bands, the Fermi level is crossed only by the band derived from the orbitals of the atoms of the outer lithium layer. We note the existence of a substantial increase in the DOS at the Fermi level relative to C_6Li, $C_6Li_{\alpha\alpha}$, and $C_6Li_{\alpha\beta}$. Analysis of the PDOS, projected on the carbon states and lithium states, reveal that the main contribution to the total DOS results mainly from the carbon muffin-tin and interstitial regions.

In the case of the Li-intercalated system denoted by $C_6Li_\alpha C_6Li_\beta C_6$, the interlayer bands are not occupied, and superconductivity is suppressed in this material, as we will demonstrate in Section V by the computating the electron-phonon coupling and estimating the superconducting transition temperature. The energy bands and DOS for this system are given in the supplementary material.

V. VIBRATIONAL MODES AND ELECTRON-PHONON COUPLING

In Section IV we found that only Li-covered graphene systems exhibit a coexistence of graphitic π-states and lithium-derived s-states at the Fermi level. We also noted that c-

direction confinement produced by the graphene layers push the bands derived from inner lithium atoms to energies well above the Fermi level. This means that only one Li-derived band crosses the Fermi level regardless of the number of Li-covered graphene layers. In addition, the total density of states at the Fermi energy in Li-covered graphene systems increases as the number of lithium layers increase, a fact that could be relevant for the enhancement of the electron-phonon coupling strength. However, when the number of Li layers is large, the Li-covered graphene system, with equal number of Li and graphene layers, begins to look like stage-1 Li GIC, which is not a superconductor. We conclude that there is an optimal number of Li layers which leads to the highest possible T_C in these systems. To this end, we present in this section electron-phonon coupling calculations for various Li-covered graphene systems, as well as the Li-intercalated graphene bilayer.

The phonon dispersion curves for Li-covered and Li-intercalated graphene systems can be divided into three regions: a high energy region ($\omega_{\mathbf{q}\nu} > 830\ cm^{-1}$) composed of in-plane carbon-vibration (C_{xy}), an intermediate region ($430\ cm^{-1} < \omega_{\mathbf{q}\nu} < 830\ cm^{-1}$) composed of out-of-plane carbon-vibration (C_z), and a low energy region ($\omega_{\mathbf{q}\nu} < 430\ cm^{-1}$) mostly composed of in-plane (Li_{xy}) and out-of-plane (Li_z) vibrations. It turns out that the low energy branches related to Li_{xy} and Li_z, and their mixture with C_z, make the greatest contribution to the electron-phonon coupling parameter.

In Figure 5 we present the phonon dispersion curves and the phonon density of states (PHDOS) in the Li-covered graphene systems C_6Li and $C_6Li_{\alpha\beta}$, and the Li-intercalated graphene bilayer C_6LiC_6. In the case of C_6LiC_6, the lowest energy branch is hardened compared C_6Li. Going from C_6Li to $C_6Li_{\alpha\beta}$, the lowest energy branch (corresponding to Li_{xy}-vibrations) in the ΓK direction is softened, while branches immediately above (corresponding to Li_z) are hardened. We also note that the lowest energy branch in $C_6Li_{\alpha\beta\gamma}$ (shown in the supplementary material) is slightly hardened relative to $C_6Li_{\alpha\beta}$; this may explain the fact that the electron-phonon coupling is stronger in $C_6Li_{\alpha\beta}$ than in $C_6Li_{\alpha\beta\gamma}$, as we will see shortly. As a final note, we do not observe any significant effect on the high energy branches due to the increasing number of Li layers in Li-covered graphene systems.

The Eliashberg function $\alpha^2F(\omega)$, plotted in Figure 6, gives the contribution of each frequency to the total electron-phonon coupling constant λ (see Sec. III). In all cases we observe a considerable contribution to the total electron-phonon coupling from the carbon-

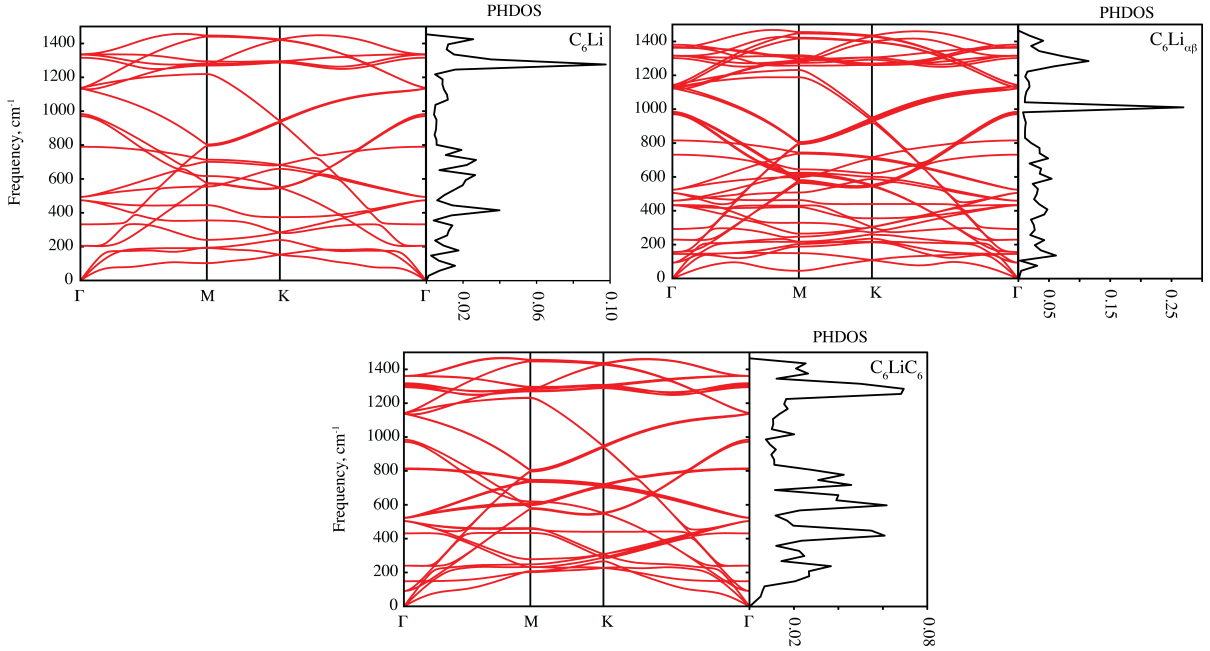

FIG. 5: (Color online) Phonon frequency dispersion and phonon density of states of C_6Li (top left), $C_6Li_{\alpha\beta}$ (top right), and C_6LiC_6 (bottom).

carbon stretching modes, which are high in energy ($\omega_{\mathbf{q}\nu} > 1000\ cm^{-1}$). More importantly, a substantial contribution to the electron-phonon coupling from the Li modes and C out-of-plane vibrational modes is observed in all the Li-covered graphene systems. However, in the case of $C_6Li_{\alpha\beta}$ this contribution is significantly larger than that in C_6Li, $C_6Li_{\alpha\alpha}$, and $C_6Li_{\alpha\beta\gamma}$ (the last two are shown in the supplementary material). For completeness' sake, we also show the Eliashberg function for C_6LiC_6 where we notice a weak coupling of electrons to the Li modes and C out-of-plane modes. This weak contribution in the Li-intercalated graphene bilayer is detrimental to the overall electron-phonon coupling parameter λ, which was calculated to be 0.29.

The calculated total electron-phonon coupling parameter λ for C_6Li is 0.55 with an estimated T_c of 6.67 K. In the case of $C_6Li_{\alpha\alpha}$ we calculated λ =0.65 and T_c=10.88K, for $C_6Li_{\alpha\beta}$ we obtained λ =0.86 and T_c=13.54 K, and for $C_6Li_{\alpha\beta\gamma}$ we found that λ is 0.57 and the estimated T_c is 8.41 K. The results of the electron-phonon coupling calculations are summarized in Table II.

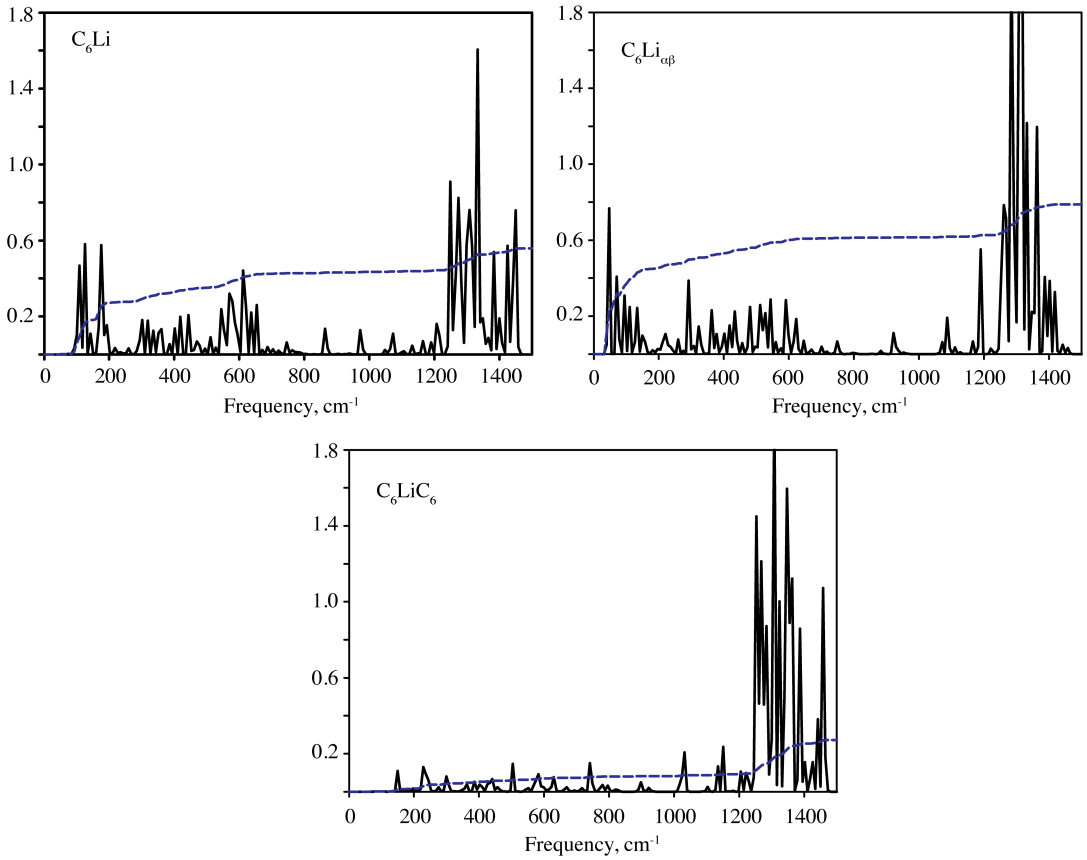

FIG. 6: (Color online) Eliashberg function $\alpha^2F(\omega)$ (continuous black line) and integrated electron-phonon coupling parameter $\lambda(\omega)$ (blue dashed line) for C_6Li (top left), $C_6Li_{\alpha\beta}$ (top right), and C_6LiC_6 (bottom).

TABLE II: Summary of the electron-phonon coupling parameter (λ), logarithmic average frequency (ω_{log}) and T_c for all the studied systems.

Structure	λ	ω_{log} (cm^{-1})	T_c (K)	Structure	λ	ω_{log} (cm^{-1})	T_c (K)
C_6Li	0.55	320.4	6.67	$C_6Li_{\alpha\beta}$	0.86	194.3	13.54
$C_6Li_{\alpha\alpha}$	0.65	308.2	10.88	$C_6Li_{\alpha\beta\gamma}$	0.57	357.8	8.41
$C_6Li_{\alpha\alpha\alpha}$	0.56	296.7	6.60	$C_6Li_{\alpha\beta\gamma\alpha}$	0.46	469.0	3.22
$C_6Li_{\alpha\alpha\alpha\alpha}$	0.49	373.4	4.56	C_6LiC_6	0.29	898.4	0.171

VI. CONCLUSIONS

In this work, we presented the results of calculations of the electronic structure and electron-phonon interaction for several configurations of graphene-lithium systems. We

assessed the structural stability and the strength of the electron-phonon coupling with respect to the stacking sequence and number of layers of lithium adatoms and the graphene sheets. We found that in all studied cases, the structures were stable, but the ones that yield the lowest energy were those where the Li adatom would sit in equivalent hollow sites; that is, with Li stacking of the form $\alpha\alpha$, $\alpha\alpha\alpha$, and $\alpha\alpha\alpha\alpha$. Structural stability of the systems was later confirmed with the calculation of the phonon dispersion curves, which do not show the presence of any imaginary frequencies. We found that, in contrast to the corresponding GICs, Li-covered graphene systems exhibit an incomplete charge transfer from the lithium atoms to the graphene planes, giving rise to a lithium-derived band which crosses the Fermi level simultaneously with graphitic π-bands. This enhances the electron-phonon coupling strength, which was found to be highest for the structure $C_6Li_{\alpha\beta}$. The calculated λ for this structure was found to be 0.86 with an average logarithmic frequency $\omega_{log} = 194.3$ cm^{-1} and a critical superconducting transition temperature $T_c = 13.54$ K. The optimal value of T_C is thus obtained for a system consisting of two graphene layers and two lithium layers.

One of the authors (RAJ) gratefully acknowledges support by NSF under grant No. HRD-0932421. DMG would like to thank the CSULA-MORE programs and CSU-LSAMP fellowship for their support under grant No. HRD-1026102-518741.

---

[1] K. S. Novoselov, A. K. Geim, S. V. Morozov, D. Jiang, Y. Zhang, S. V. Dubonos, I. V. Grigorieva, and A. A. Firsov, Electric Field Effect in Atomically Thin Carbon Films, Science **306**, 5696 (2004).

[2] M. I. Katsnelson, K. S. Novoselov, and A. K. Geim, Chiral tunnelling and the Klein paradox in graphene, Nature Physics **2**, 620 (2006).

[3] K. S. Novoselov, Z. Jiang, Y. Zhang, S. V. Morozov, H. L. Stormer, U. Zeitler, J. C. Maan, G. S. Boebinger, P. Kim, and A. K. Geim, Room-Temperature Quantum Hall Effect in Graphene, Science **315**, 1379 (2007).

[4] Y. Zhang, Y. W. Tan, H. L. Stormer, P. Kim, Experimental observation of the quantum Hall effect and Berry's phase in graphene, Nature **438**, 201 (2005).

[5] R. R. Nair, P. Blake, A. N. Grigorenko, K. S. Novoselov, T. J. Booth, T. Stauber, N. M. R.

Peres, and A. K. Geim, Fine Structure Constant Defines Visual Transparency of Graphene, Science **320**, 1308 (2008).

[6] A.H.C. Neto, F. Guinea, N.M.R. Peres, K.S. Novoselov, and A.K. Geim, The electronic properties of graphene, Rev. Mod. Phys. **81**, 109 (2009).

[7] N. B. Hannay, T. H. Geballe, B. T. Matthias, K. Andres, P. Schmidt and D. MacNair, Superconductivity in Graphitic Compounds, Phys. Rev. Lett. **14**, 255 (1965).

[8] Y. Koike and S. Tanuma, Superconductivity in the graphite-potassium intercalation compound C_8K, J. Phys. Chem. Solids **41**, 1111 (1980).

[9] M. Kobayashi and I. Tsujikawa, Susceptibility Fluctuation in Superconducting First Stage Potassium Graphite Intercalation Compound near Transition Temperature, J. Phys. Soc. Jpn. **46**, 1945 (1979).

[10] M. G. Alexander, D. P. Goshorn, D. Gurard, P. Lagrange, M. El Makrini and D. G. Onn, Superconductivity of the graphite intercalation compounds $KHgC_8$ and $RbHgC_8$: Evidence from specific heat, Solid State Commun. **38**, 103 (1981).

[11] Y. Iye and S. Tanuma, Superconductivity of graphite intercalation compounds with alkali-metal amalgams, Phys. Rev. B **25**, 4583 (1982).

[12] R. Al Jishi, Model for superconductivity in graphite intercalation compounds, Phys. Rev. B **28**, 112 (1983).

[13] N. Emery, C. Herold, J.-F. Mareche, and P. Lagrange, Synthesis and superconducting properties of CaC_6, Sci. Technol. Adv. Mater. **9**, 044102 (2008).

[14] T. E. Weller, M. Ellerby, S. S. Saxena, R. P. Smith and N. T. Skipper, Superconductivity in the Ytterbium Intercalated Graphite Compounds C_6Yb and C_6Ca, Nature Physics **1**, 39 (2005).

[15] N. Emery, C. Herold, M. dAstuto, V. Garcia, Ch. Bellin, J. F. Mareche, P. Lagrange, and G. Loupias, Superconductivity of Bulk CaC_6, Physical Review Letters **95**, 087003 (2005).

[16] A. C. Walters, C. A. Howard, M. H. Upton, M. P. M. Dean, A. Alatas, B. M. Leu, M. Ellerby, D. F. McMorrow, J. P. Hill, M. Calandra, F. Mauri, Comparative study of the phonons in non-superconducting BaC_6 and superconducting CaC_6 using inelastic x-ray scattering, arXiv:1102.4767v1 [cond-mat.supr-con], (2011).

[17] R. Ricardo da Silva, J. H. S. Torres, and Y. Kopelevich, Indication of Superconductivity at 35 K in Graphite-Sulfur Composites, Phys. Rev. Lett. **87**, 147001 (2001).

[18] S. Moehlecke, Y. Kopelevich, and M. B. Maple, Interaction between superconducting and ferromagnetic order parameters in graphite-sulfur composites, Phys. Rev. B **69**, 134519 (2004).

[19] S. De Franceschi, L. Kouwenhoven, Ch. Schönenberger and W. Wernsdorfer, Hybrid superconductor-quantum dot devices, Nature Nanotechnology **5**, 703 (2010).

[20] M. Huefner, C. May, S. Kicin, K. Ensslin, T. Ihn, M. Hilke, K. Suter, N. F. de Rooij, and U. Staufer, Scanning gate microscopy measurements on a superconducting single-electron transistor, Phys. Rev. B **79**, 134530 (2009).

[21] J. Delahaye, J. Hassel, R. Lindell, M. Sillanpää, M. Paalanen, H. Seppä, and P. Hakonen, Low-noise current amplifier based on mesoscopic Josephson junction, Science **299**, 1045 (2003).

[22] B. Uchoa and A. H. Castro Neto, Superconducting States of Pure and Doped Graphene, Phys. Rev. Lett. **98**, 146801 (2007).

[23] E. Zhao and A. Paramekanti, BCS-BEC Crossover on the Two-Dimensional Honeycomb Lattice, Phys. Rev. Lett. **97**, 230404 (2006).

[24] A.M. Black-Schaffer and S. Doniach, Resonating valence bonds and mean-field d-wave superconductivity in graphite, Phys. Rev. B **75**, 134512 (2007).

[25] C. Honerkamp, Density Waves and Cooper Pairing on the Honeycomb Lattice, Phys. Rev. Lett. **100**, 146404 (2008).

[26] N. B. Kopnin and E. B. Sonin, BCS Superconductivity of Dirac Electrons in Graphene Layers, Phys. Rev. Lett. **100**, 246808 (2008).

[27] J. Gonzalez, Kohn-Luttinger superconductivity in graphene, Phys. Rev B **78**, 205431 (2008).

[28] V. M. Loktev and V. Turkowski, Suppression of the superconducting transition temperature of doped graphene due to thermal fluctuations of the order parameter, Phys. Rev. B **79**, 233402 (2009).

[29] R. A. Jishi, M. S. Dresselhaus, and A. Chaiken, Theory of the upper critical field in graphite intercalation compounds, Phys. Rev. B **44**, 10 248 (1991).

[30] R. A. Jishi and M. S. Dresselhaus, Superconductivity in graphite intercalation compounds, Phys. Rev. B **45**, 12465 (1992).

[31] R. A. Jishi, D. M. Guzman, H. M. Alyahyaei, Theoretical Investigation of Two-Dimensional

Superconductivity in Intercalated Graphene Layers, Adv. Studies Theor. Phys. **5**, 703 (2011).

[32] G. Profeta, M. Calandra, F. Mauri, Phonon-mediated superconductivity in graphene by lithium deposition, Nature Physics **8**, 131 (2012).

[33] K. Sugawara, K. Kanetani, T. Sato, and T. Takahashi, Fabrication of Li-intercalated bilayer graphene, AIP Advances **1**, 022103 (2011).

[34] P. Blaha, K. Schwarz, G. K. H. Madsen, D. Kavasnicka, and J. Luitz, WIEN2K: *An Augmented Plane Wave+Local Orbitals Program for Calculating Crystal Properties* (Technische Universität, Wien, Austria, 2001).
`http://www.wien2k.at`.

[35] J. P. Perdew, K. Burke, and M. Ernzerhof, Generalized Gradient Approximation Made Simple, Phys. Rev. Lett. **77**, 2865 (1996).

[36] P. Giannozzi *et al.*, QUANTUM ESPRESSO: a modular and open-source software project for quantum simulations of materials, J. Phys. Condens. Matter **21**, 395502 (2009).

[37] P. B. Allen and R. C. Dynes, Transition temperature of strong-coupled superconductors reanalyzed, Phys. Rev. B **12**, 905 (1975).

[38] W. L. McMillan, Transition Temperature of Strong-Coupled Superconductors, Phys. Rev. **167**, 331 (1968).

[39] P. Morel and P. W. Anderson, Calculation of the Superconducting State Parameters with Retarded Electron-Phonon Interaction, Phys. Rev. **125**, 1263 (1962).

[40] R.F.W. Bader, *Atoms in Molecules: A Quantum Theory* (Oxford University Press, Oxford, 1990).

[41] G. Csányi, P. B. Littlewood, Andriy H. Nevidomskyy, Chris J. Pickard, and B. D. Simons, The role of the interlayer state in the electronic structure of superconducting graphite intercalated compounds, Nature Physics **1**, 42 (2005).

[42] M. Calandra and F. Mauri, Theoretical Explanation of Superconductivity in C_6Ca, Phys. Rev. Lett. **95**, 237002 (2005).

[43] M.S. Dresselhaus and G. Dresselhaus, Intercalation Compounds of Graphite, Adv. Phys. **51**, 1 (2002).